

Rotational predissociation resonances in anharmonic potentials

J. Recamier

*Laboratorio Cuernavaca, Instituto de Física, Universidad Nacional Autónoma de México
Apartado postal 48-3, 62251 Cuernavaca, Mor., Mexico*

M. Berrondo

*Department of Physics and Astronomy Brigham Young University
Provo, UT 84602*

Recibido el 10 de septiembre de 1997; aceptado el 6 de mayo de 1998

We calculate the resonant energies for finite range, anharmonic, potentials. We exemplify our method with the well known Morse potential and with a potential given by Deng [1] both of them with a centrifugal barrier. In this work we calculate the resonant energies using Siegert boundary conditions [2]. Starting with a complex wavenumber k , we integrate numerically from the origin up to a matching point using Numerov's method. The inward integration is performed using the corresponding Riccati equation. The complex eigenvalues are found by matching the two logarithmic derivatives. We find narrow shape resonances within the well, above the dissociation limit, as well as broad resonances above the centrifugal barrier and anti-bound states.

Keywords: Resonances; Morse; numerical calculation

Calculamos las energías de resonancias para potenciales anarmónicos de alcance finito. Ejemplificamos nuestro método con el bien conocido potencial de Morse y con un potencial propuesto por Deng, ambos con barrera centrífuga. Para calcular las energías de las resonancias, partimos de un número de onda complejo k e integramos de forma numérica desde el origen hasta un punto de traslape utilizando el método de Numerov. La integración hacia adentro se hace usando la ecuación de Riccati correspondiente. Los valores propios, complejos, son encontrados al empatar las dos derivadas logarítmicas. Encontramos resonancias delgadas en el pozo por encima del límite de disociación y resonancias anchas por encima de la barrera centrífuga, así como estados anti-ligados.

Descriptores: Resonancias; Morse; cálculos numéricos

PACS: 03.65.-w; 03.65.Nk; 30.34

1. Introduction

The Morse potential has been used frequently to describe chemical bonds since, in contrast with the harmonic oscillator model, it has a finite number of bound states allowing the possibility of dissociation at high enough excitation energies, and also because it takes into account the quasi-harmonic behavior of the bond in the vicinity of the potential minimum. The analytical solution of the Schrödinger equation with a Morse potential has been known for a long time [3, 4]. However, in these solutions it was necessary to extend the domain of the radial coordinate to the non-physical region of negative values. This is a result of the fact that the Morse potential attains a finite value when the radial coordinate goes to zero. Recently, a study of the relevance of this approximation for the evaluation of Frank Condon factors was done showing that the effects are indeed small [5]. The potential proposed by Deng also has analytical solution for the case of zero angular momentum and has as an advantage over the Morse potential the fact that it does go to infinity as the radial coordinate approaches zero. Thus, the domain of the radial coordinate does not need to be extended to the unphysical region. In this work we make a comparison between the bound, resonant and anti-bound states of a Morse potential and a Deng

potential for several values of the potential's depth and of the angular momentum.

The addition of a rotational term to a diatomic molecule potential produces a barrier allowing for tunneling and the subsequent predissociation of the molecule. The energies at which the tunneling is enhanced are the resonant energies. Resonant or quasibound *states* are defined as the solutions of Schrödinger's equation for the corresponding potential with purely outgoing wave boundary conditions asymptotically, and regular at the origin [6–8].

The associated eigenvalues of the nonhermitian problem correspond to the complex poles of the S -matrix, with the real part representing the position of the resonance, and the imaginary part giving the inverse lifetime. The resonant states are associated to the residues of the Green function at those poles [9]. Contrary to the case of bound states, resonant states diverge exponentially for large distances making approximation methods awkward to apply.

In the present paper, we apply a method based upon the combination of the usual radial equation and Riccati's equation [2]. We start by choosing a matching radius r_m dividing the space into two parts. Integrating the radial equation in the inner region presents no problem since we are far away from the region where the solution diverges. In the outer region, on

the other hand, we transform the radial equation to the Riccati form and integrate it as a nonlinear first order equation. We do not continue the integration into the inner region due to the presence of nodes of the wave function [10, 11]. Matching logarithmic derivatives at r_m gives the resonant energies. We present the complex energies corresponding to shape resonances for the two potentials mentioned above.

In the next Section we present the use of the Riccati equation to calculate the resonant energies, then, a description of the numerical integration methods used and finally we present our numerical results and a brief discussion.

2. Resonances

An important phenomenon in scattering is the occurrence of resonances in the scattering cross section. In the neighborhood of a resonance, the cross sections for all allowed reactions and for elastic scattering show pronounced peaks as the incident energy is varied. All these peaks have nearly identical shapes, and the angular distributions for these processes generally have simple shapes characteristic of the angular momentum associated with the resonance.

These observations can be interpreted as arising from long-lived virtual states of the compound system that are formed when the projectile and the target coalesce. The enhanced cross section is a result of the greater probability of interacting when such long lived states can be formed, and the widths of the peaks are associated with the finite lifetimes of these states, via the uncertainty relation $\Delta E \Delta t \approx \hbar$.

A resonant state is defined as a solution of Schrödinger's equation fulfilling Siegert's boundary condition [1-4]. For the case of spherically symmetric potentials $V(r)$ with a finite range, this corresponds to the asymptotic condition for the radial wave function $\psi(r)$ as $r \rightarrow \infty$:

$$\frac{\psi'(r)}{\psi(r)} \rightarrow ik, \quad (1)$$

where k is the (complex) wave number.

These states include bound states as well as proper resonant states, representing purely outgoing waves, with no incoming component. Although, strictly speaking, these conditions are nonphysical, the complex energies associated to these states give a very good description of the resonant energies and their lifetimes.

The radial equation for an effective potential $V_J(r)$ with angular momentum J is given as

$$\psi''(r) + [k^2 - V_J(r)]\psi(r) = 0, \quad (2)$$

in natural units, $\hbar = 2m = 1$. Its numerical integration for proper resonant states, however, becomes unstable asymptotically. This is due to the fact that the boundary condition Eq. (1) implies an exponentially growing behavior with r . The correct solution becomes contaminated with the exponentially small component asymptotically.

In the case of bound states, k in Eq. (1) is imaginary positive [8], the wave function decays exponentially with r ,

and the integration can be started from the asymptotic region inwards. In practice, we also integrate outwards from the origin and find the correct eigenvalue by matching logarithmic derivatives of the wave functions at an intermediate point [11].

An alternative to the use of Eq. (2) is to transform this radial equation into a first order nonlinear form, namely Riccati's equation. Defining

$$g(r) = \frac{\psi'(r)}{\psi(r)}, \quad (3)$$

Eq. (2) becomes

$$g'(r) + g^2(r) + E - V_J(r) = 0, \quad (4)$$

where $E = k^2$ is the complex energy eigenvalue. The purely outgoing wave boundary condition for $g(r)$ is simply:

$$g(r) \rightarrow ik. \quad (5)$$

Eq. (4) can now be integrated inwards starting from the constant ik . A new problem arises now from the fact that $g(r)$ diverges at the nodal points of $\psi(r)$.

In the present work we integrate Eq. (2) from the origin up to a matching point r_m , and Eq. (4) from the asymptotic region inwards, down to the same point r_m . The matching point is chosen in such a way that we do not find any nodes of $\psi(r)$ during the integration of Riccati's equation. The complex eigenvalues corresponding to the resonant states are determined matching the logarithmic derivative of the internal solution with the external solution of the Riccati equation:

$$\frac{\psi'(r_{m-})}{\psi(r_{m-})} = g(r_{m+}). \quad (6)$$

3. Numerical integration

The potentials we considered in this work had well depth A and minimum at $r = r_0$. For the Morse case, the effective potential is given by:

$$V_J(r) = A \left[e^{-2(r-r_0)} - 2e^{-(r-r_0)} \right] + \frac{J(J+1)}{r^2}, \quad (7)$$

while for the Deng case:

$$V_J(r) = A \left[\frac{b^2}{(e^r - 1)^2} - \frac{2b}{e^r - 1} \right] + \frac{J(J+1)}{r^2}, \quad (8)$$

with $b = e^{r_0} - 1$, and we have included the centrifugal potential corresponding to a molecular rotation with angular momentum J . The centrifugal term creates a hump in the effective potential, allowing for resonant states with positive energy, besides the ordinary bound states corresponding to negative energies. Using the procedure described above, we integrate Eqs. (2) and (4) numerically and determine the energy eigenvalues.

The outward integration of the Schrödinger equation is performed using Numerov's method on a discrete mesh from $r = 0$ to the matching point $r = r_m$. For Riccati's equation,

TABLE I. Energy eigenvalues for the first two states of a Morse and a Deng potential with fixed depth $A = 4$ and several values of the angular momentum J .

$n = 0$				
J	Morse	Deng	ΔE	
0	-2.25000	-2.22216	-0.02784	
1	-2.14404	-2.11672	-0.02732	
2	-1.93403	-1.90769	-0.02634	
3	-1.62393	-1.59894	-0.02499	
4	-1.22009	-1.19671	-0.02338	
5	-0.73196	-0.71033	-0.02163	
$n = 1$				
J	Morse	Deng	ΔE	
0	(-0.25000, 0.00000)	(-0.23192, 0.00000)	(0.01808, 0.00000)	
1	(0.03318, -0.51687)	(0.03812, -0.52314)	(-0.00494, 0.00627)	
2	(0.09353, -0.53729)	(0.09819, -0.54312)	(-0.00466, 0.00583)	
3	(0.18415, -0.56717)	(0.18820, -0.57234)	(-0.00405, 0.00517)	
4	(0.30150, -0.60546)	(0.30472, -0.60959)	(-0.00322, 0.00413)	
5	(0.43857, -0.64690)	(0.44128, -0.64960)	(-0.00271, 0.00270)	

on the other hand, we use a fourth order Runge-Kutta method. At the starting point for this integration, $r = R$, we choose the initial value $g_J(R)$ as:

$$g_J(R) = k \frac{\hat{h}'_J(kR)}{\hat{h}_J(kR)}, \tag{9}$$

where \hat{h}_J represents the Riccati-Hankel function (+) of order J , and the ' denotes the derivative with respect to the argument. This is the asymptotic form for the solution with purely outgoing wave character in the case of an asymptotically vanishing potential.

We determine the complex wave number k using a Newton-Raphson procedure for Eq. (6). The resonance energy is given as $E = k^2$. The matching point is chosen to the right of the classical turning point for bound states. In the case of proper resonant states, r_m is to the left of the effective potential maximum, both for resonances below and above the potential barrier.

In order to validate our integration procedure, we solved the case of a square potential well of depth U and step at $r = 1$, for $l = 0, 1$, and 2 , and compared with the solutions of the transcendental equation:

$$\kappa \frac{\hat{j}'_l(\kappa)}{\hat{j}_l(\kappa)} = k \frac{\hat{h}'_l(k)}{\hat{h}_l(k)}, \tag{10}$$

where

$$\kappa = \sqrt{k^2 + U}, \tag{11}$$

and \hat{j}_l is the Riccati-Bessel function of order l .

The numerical values for the resonant energies were obtained matching at $r_m = 1$ in this case. Using Mathematica we solved Eq. (10) for several values of U and found that with our integration procedure we have an accuracy of one part in 10^5 .

4. Numerical results and discussion

In order to model the rotational predissociation of a molecule, we choose a Morse and a Deng potentials with different values of A , and with their minimum located at $r_0 = 4$. The initial point in the numerical integration of Eq. (4) is taken as $R = 16$, in the present units.

For $J = 0$ there are no resonances. The bound state energies corresponding to the one-dimensional Morse oscillator are given by [12]:

$$E_n = -(\sqrt{A} - n - 1/2)^2. \tag{12}$$

Our numerical integration gives excellent results in this case. For the case of the Deng potential we used the same parameters as in the Morse case.

In Table I we show the energies for the first and second poles for $0 \leq J \leq 5$, with well depth $A = 4$ fixed. For this value of the potential's depth there are not only bound but also resonant states. For the first pole we see that the Morse potential binds more strongly than the Deng potential, the difference between the two is a decreasing function of the angular momentum J . The differences are small, less than 1% for this pole. For the second pole we found a bound state with $J = 0$ which is again more tightly bound for the Morse case, and resonant states for all other values of the angular momentum. As for the case of bound states, the differences in the energies of the resonances between the two model potentials are a decreasing function of the angular momentum, the relative magnitude of these differences is larger than in the bound state case being of the order of up to 10%.

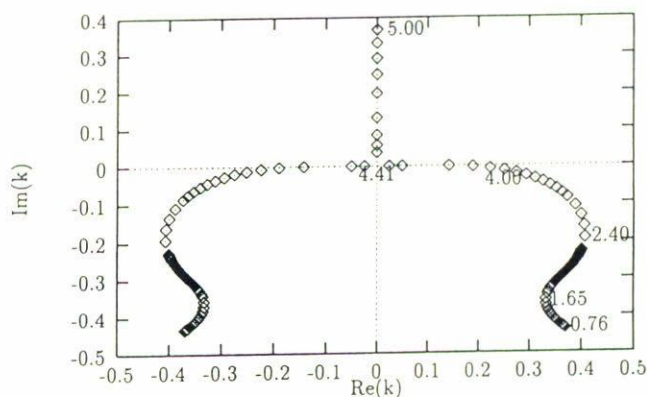
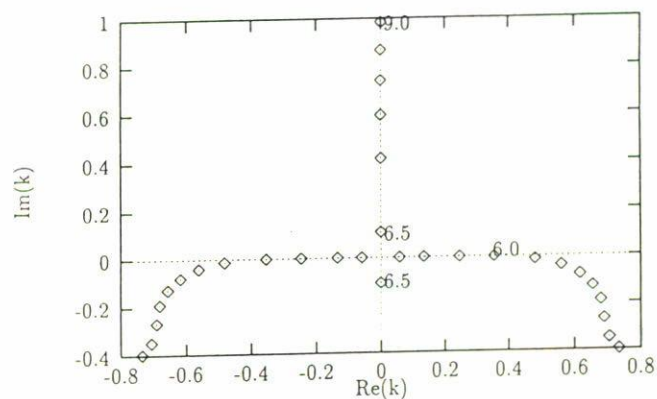
In Table II we present the energies of the first three poles for the two model potentials considered with $0 \leq J \leq 5$ and well depth $A = 9$ fixed. For $J = 1$ we notice that the first three states are bound, higher states are resonant states. As we increase the rotational quantum number J , the energies of the bound states become less negative and approach positive values. For instance, the third state, which is bound

TABLE II. Energy eigenvalues E_n , $n = 0, 1, 2, 3$ for a Morse and a Deng potential with fixed depth $A = 9$, and several values of the angular momentum J .

	$n = 0$		$n = 1$	
	Morse	Deng	Morse	Deng
$J = 0$	(-6.25000, 0.00000)	(-6.20351, 0.00000)	(-2.25000, 0.00000)	(-2.18573, 0.00000)
$J = 1$	(-6.13732, 0.00000)	(-6.09118, 0.00000)	(-2.16498, 0.00000)	(-2.10157, 0.00000)
$J = 2$	(-5.91273, 0.00000)	(-5.86726, 0.00000)	(-1.99615, 0.00000)	(-1.93445, 0.00000)
$J = 3$	(-5.57777, 0.00000)	(-5.53325, 0.00000)	(-1.74599, 0.00000)	(-1.68682, 0.00000)
$J = 4$	(-5.13479, 0.00000)	(-5.09143, 0.00000)	(-1.41845, 0.00000)	(-1.36259, 0.00000)
$J = 5$	(-4.54495, 0.00000)	(-4.58702, 0.00000)	(-0.96753, 0.00000)	(-1.01929, 0.00000)
	$n = 2$		$n = 3$	
	Morse	Deng	Morse	Deng
$J = 0$	(-0.25000, 0.00000)	(-0.22319, 0.00000)	--	--
$J = 1$	(-0.20292, 0.00000)	(-0.17760, 0.00000)	(0.07690, -0.55843)	(0.08630, -0.56794)
$J = 2$	(-0.11257, 0.00000)	(-0.09046, 0.00000)	(0.13026, -0.57547)	(0.13940, -0.58458)
$J = 3$	(0.00999, -0.00003)	(0.02518, -0.00068)	(0.21091, -0.60039)	(0.21963, -0.60894)
$J = 4$	(0.14506, -0.02380)	(0.15539, -0.03045)	(0.31788, -0.63263)	(0.32589, -0.64034)
$J = 5$	(0.30804, -0.08925)	(0.31487, -0.10009)	(0.44838, -0.67066)	(0.45568, -0.67714)

for $J = 0, 1$, and 2 becomes a resonant state for $J = 3$. Its real part in the complex energy plane is nearly zero and it takes larger values as we increase the angular momentum J . With respect to the imaginary part of the pole, we see that for $J = 3$ it is of the order of 1×10^{-4} which is the numerical accuracy of this calculation, for larger values of J it becomes more negative indicating a wider resonance and correspondingly a shorter lived state. All resonant states considered in this table behave in a similar form, the real part of their energies increasing with the angular momentum and their imaginary parts going towards $-\infty$ as the rotational barrier increases. These general features apply to both model potentials. The behavior of the poles as a function of the well depth is not so simple. In Fig. 1 we show the trajectory of the first poles ($n = \pm 1$) in the complex k -plane for a fixed value of the angular momentum $J = 3$ and several values of A for the Deng potential. Since both poles are symmetrical about the imaginary axis we discuss the evolution of only one of them. We notice that for small values of A there are no bound states (corresponding to a positive imaginary k), and the pole has a large negative imaginary part, as the well's depth is increased the imaginary part of the pole diminishes, its width becomes smaller and the state has a larger lifetime, this kind of behavior is similar to the one observed in the case of a square well potential and for the Morse potential [2]. Notice however that the behavior of the real part of the pole is more complicated. First it decreases with increasing A , then it turns back and finally, for large enough values of A , it decreases again going towards the imaginary axis. We believe that this behavior is due to the asymmetry of the potential.

In Fig. 2 we show the behavior of the pole ($n = 1$) for angular momentum $J = 5$ and different values of the well's depth. As in the previous case, for small values of A there are only resonant states with a large imaginary part indicating a short lived state. As the well depth is increased, the imaginary part of the pole diminishes until it attains the real axis. We

FIGURE 1. Complex second pole trajectory in the k -plane for a Deng potential with angular momentum $J = 3$ varying the depth A . Selected values of A are shown.FIGURE 2. Complex second pole trajectory in the k -plane for a Deng potential with angular momentum $J = 5$ varying the depth A . Selected values of A are shown.

notice that the value of the well's depth for which this happens is larger for $J = 5$ than its value for $J = 3$. Continuing

the increase in the values of A , we get to a point where the two poles coalesce at the origin, giving rise to a double pole. For even larger values of A this double pole splits into a pair of poles moving in opposite directions along the imaginary axis, *i.e.* a bound state and an anti bound state (ABS).

5. Antibound states

Antibound states have an exponentially growing behavior asymptotically along the radial direction. The corresponding energy eigenvalue is real and negative, but it is located in the second Riemann sheet of the complex E -plane [7]. These states show up experimentally as an anomalously large value of the cross section for low energies. The classical example of this kind of behavior appears in the low energy end of proton-neutron scattering. The singlet “deuteron” state turns out to be unbound and appears only as an ABS.

For the present case of a Deng potential, we have not found true resonances for $J = 0$. Apparently the hump in the effective potential for $J \neq 0$ is necessary in order to obtain a constructive interference within the well, even in the case of very sharp resonances with energies *above* the potential barrier (see Table I). On the other hand, for the Morse case

with $J = 0$ (pure Morse potential with no hump) there are no resonances, but only bound and antibound states. The pole trajectory in this case is a straight line along the imaginary k -axis moving from positive to negative values as we *decrease* the value of A . We can easily understand this behavior [13] from the exact solution of the 1-d Morse potential, Eq. (12). The complex momentum of Siegert states is given as:

$$k = i(\sqrt{A} - n - 1/2). \quad (13)$$

Values of $A < (n + 1/2)^2$ present a negative imaginary part, corresponding to ABS. Indeed, for shallow wells, there are no bound states for $0 < A < 1/4$. Instead, the “zero-point” vibration manifests itself as an antibound state for $J = 0$. The corresponding cross section is anomalously large at the threshold in this case.

Acknowledgments

One of us (MB) would like to thank the Instituto de Física, UNAM, for its hospitality and, in particular, the “Cátedra Elena Aizen de Moshinsky” for its support. This work was partially supported by CONACyT through project 4877-E.

-
1. Z.H. Deng and Y.P. Fan, *Shandong University Journal* **1** (1957) 162.
 2. M. Berrondo and J. Récamier, *International Journal of Quantum Chemistry* **62** (1997) 239.
 3. P.M. Morse, *Phys. Rev.* **34** (1929) 57.
 4. C.L. Pekeris, *Phys. Rev.* **45** (1934) 98.
 5. E. Ley-Koo, S. Mateos-Cortés, and G. Villa-Torres, *International Journal of Quantum Chemistry* **58** (1996) 23.
 6. A.F.J. Siegert, *Phys. Rev.* **56** (1939) 750.
 7. H.M. Nussenzveig, *Causality and Dispersion Relations*, (Academic Press, New York, 1972).
 8. J.R. Taylor, *Scattering Theory*, (J. Wiley, New York, 1972), Chap. 11.
 9. M. Berrondo and G. García-Calderón, *Lett. Nuovo Cimento* **20** (1977) 34.
 10. B.R. Johnson, *J. Comput. Phys.* **13** (1973) 445; B.R. Johnson, *J. Chem. Phys.* **67** (1977) 4086.
 11. O. Atabek and R. Lefebvre, *Phys. Rev. A* **22** (1980) 1817.
 12. M. Berrondo, A. Palma, and J. López-Bonilla, *IJQC* **31** (1987) 243.
 13. M. Berrondo and J. Récamier, (to be published).